J. Fluid Mech. (1987), *vol.* 175, *pp.* 395–412
Printed in Great Britain

On surface waves crossing a step with horizontal shear

By JEROME SMITH

Marine Physical Laboratory of the Scripps Institution of Oceanography, University of California, San Diego, La Jolla, CA 92093, USA

(Received 30 July 1986)

When surface waves encounter a step in bottom topography and/or a change in velocity parallel to the step, refraction and partial reflection occur. Comparison of several approximate solutions indicates that no single approximation works well for all cases. The pattern of success among models suggests that the velocity profile at the boundary favours the free wave with smaller vertical scale. For current changes over a flat bottom, a two-term Galerkin expansion (cf. Evans 1975) is employed for comparison with the other more general models. For small currents ($|\Delta V| < \frac{1}{2}c$), an 'action-based approximation' (cf. Smith 1983) is favoured, although all models perform adequately. With a strong current, one one-term (one-sided) model performs best, another worst among models; the favoured model includes ephemeral modes on the side with larger-scale free waves. For changes in depth only, the one-sided model with ephemeral modes on the deep side was shown by Miles (1967) to perform well. The two-term expansion (cf. Evans 1975) is not easily extended to this case, and none of the other approximations perform adequately. In the unusual case of a step combined with a strong current, such that much shorter waves occur in the deeper region, it is inferred that none of the models are accurate. Reflection from a submerged wall provides a severe test of the models. Without the ephemeral modes, no net reflection occurs. The Miles-like model overpredicts reflection slightly.

1. Introduction

The problem considered is that of (linear) refraction and partial reflection of surface gravity waves propagating at some angle over a discontinuity in depth, velocity, or both; flow perpendicular to the shelf is not considered. Such a discontinuity could serve, in practice, as an approximation to a change in depth and/or current over a small but finite horizontal distance. Even so, no exact solution of this simpler problem exists; rather, arbitrary accuracy can be obtained by increasing the number of terms in a numerical analysis. A practical application would probably involve integration over a spectrum of incident waves; thus, it is desirable to develop guidelines for accuracy versus the number of terms included. No such complete numerical solution is attempted here; rather, guidelines are developed by comparison of results from simpler approaches.

Several previous approximations are extended and compared within a unified framework. The pivotal distinction between the models is what vertical profile of velocity (or pressure) is assumed to exist at the boundary between the regions. In the simplest, plane-wave approximation, the free-wave profile from just one side is assumed to dominate, and the other free-wave profile is adjusted to a best fit. In a plane-wave variational approximation (after Miles 1967), the free-wave profile from

one side again dominates, while in the other region ephemeral modes (solutions that are oscillatory in depth and decay horizontally) are included in the best fit. In his analysis, Miles (1967) found this approximation to be quite accurate for a change in depth alone, with the ephemeral modes included on the deeper side. Here, this approach is extended to include current changes as well. In an Evans-like approximation (after Evans 1975), a two-term Galerkin expansion is employed; i.e. the profile at the boundary is assumed to be a linear combination of just the two free-wave profiles. The ephemeral modes on both sides are then included in the fit. Here, this approach is extended to finite depth, but is limited to a flat bottom; i.e. only a current change is treated. In a similar extension, but allowing additional terms in the profile description, McKee & Tesoriero (1986) show that this two-term expansion is adequate for the present comparison, with (for example) errors in the magnitude of the reflection of less than about 0.03 times the incident amplitude (for an incident angle of 45° with strong opposing flow), decreasing to negligible levels for ΔV less than half the phase speed of the waves. Extension of Evans' approach to include changes in depth proves cumbersome; it serves here as a reference for comparison with the other more general models.

A common theme which can be traced through the previous works is the conservation of wave action. Evans (1975) was able to show that the complete solution conserves net action flux across the change, where action is defined as the wave energy divided by frequency. For a change in depth only, conservation of action and energy are identical in form, and were shown by Miles (1967) to hold. Solutions for diffraction by a trench (Miles 1982; Kirby & Dalrymple 1983; Kirby, Dalrymple & Seo 1987) also conserve wave action. Indeed, action is conserved for a wide class of problems, including that posed here (see Hayes 1970), and therefore provides a consistency check on solutions obtained. In one recent study of diffraction by a current jet, action is not conserved (Mei & Lo 1984); however, the difficulty is traced to application of inappropriate boundary conditions (Kirby 1986). While Mei & Lo (1986) give revised results, the new conditions are not given, and it is therefore not possible to verify that they are correct.

An alternative approach is to use action conservation explicitly in formulating the model, as in my earlier 'action-based model' (Smith 1983), which was found to perform well for weak current changes ($\Delta V < \frac{1}{2}c$). This is extended here to include changes in depth. Comparison with the plane-wave solutions leads to interpretation of the action-based model as a root-mean-square matching over the open portion of the boundary. Comparison with Evans' approximation indicates that, for velocity changes smaller than half the phase speed, the action model is slightly more accurate than either possible plane-wave solution. In the limit of strong opposing currents, however, the reflection approaches that given by the plane-wave solution in which the high-wavenumber (transmission) side is treated as the shallow region. Physically, the strong surface trapping is analogous to a shallower water depth. In the case of a step only (Miles' problem), there is a negligible difference between the action and plane-wave models. Over a broad range of shelf depths, neither of these simpler models is adequate; in these cases the ephemeral modes in the deep region are important.

From the pattern of success and failure among the models, a consistent interpretation emerges: to the degree that the vertical scale of the free waves differs, the smaller-scale wave is favoured in the profile at the boundary. Thus, the region containing the larger-scale waves requires a greater contribution from ephemeral modes to meet the boundary conditions. As a guideline, enough modes should be

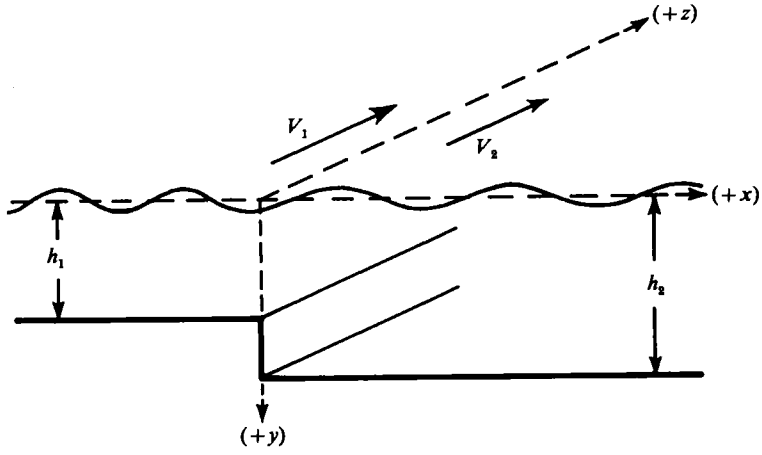

FIGURE 1. Schematic view of the problem. At $x = 0$, the depth and/or the velocity parallel to the z-axis may change. Region 1 is to the left ($x < 0$), region 2 to the right. The geometry may always be rotated so that $h_1 \leqslant h_2$.

included to resolve the change in scale from large to small. For moderately large changes in depth, for example, the number of modes needed may be large on the deep side (up to about 30 modes), and small on the shallow side (of order 1).

Finally, diffraction by a thin submerged wall is considered. Since the plane-wave and action-based models tacitly assume that only the net change in index of refraction is important, they predict no net reflection off the wall. In this case, the difficulty in matching via the ephemeral modes is a dominant effect, and so a treatment at least as sophisticated as Miles' (1967) approximation is required. In the true solution, the velocity is singular at the top of the wall (Dean 1945), whereas the present application of Miles' approximation imposes the profile of free waves in the non-existent middle region. The resulting errors in reflection typically amount to about 0.035 times the incident amplitude.

2. Formulation

The formulation here follows closely those of Miles (1967), Evans (1975) and Smith (1983). Interested readers are referred to these for more details.

The problem is posed in terms of velocity potentials in each of two inviscid, irrotational regions, and consists of matching interior solutions for wavelike motion in each region at a boundary characterized by an abrupt change in depth and/or tangential velocity (i.e. velocity parallel to the step). The axes are chosen as in Miles: the change occurs at $x = 0$, y increases downwards, and z is parallel to the step/vortex sheet (see figure 1). Each region has a flat bottom, at depths h_1 for $x < 0$, and h_2 for $x > 0$. Without loss of generality, it is assumed that $h_1 \leqslant h_2$. Thus, let

$$\Phi_n = V_n z + \phi(x, y, z, t), \quad n = \begin{cases} 1 & (x < 0) \\ 2 & (x > 0) \end{cases} \tag{2.1}$$

be the total velocity potential in each region. Assuming wave motion of the form $\exp \mathrm{i}(pz - \omega t)$, the intrinsic frequency in each region is defined by

$$\sigma_n \equiv \omega - pV_n, \tag{2.2}$$

(where ω is the apparent frequency and p is the along-step component of the wavenumber). In the following discussion, $V_n > 0$ (i.e. current flowing in the same sense as the z-propagation of the waves) is referred to as a following current and $V_n < 0$ as an opposing current.

The interior solutions are (cf. Miles 1967):

$$\phi_n = (\operatorname{sgn} x)\left\{(A_n \mathrm{e}^{-\mathrm{i}q_n|z|} + B_n \mathrm{e}^{\mathrm{i}q_n|z|})\,\chi_n(y) + \sum_{j=1}^{\infty} C_{nj}\,\mathrm{e}^{-r_{nj}|z|}\psi_{nj}(y)\right\}, \tag{2.3}$$

where

$$\chi_n(y) = 2k_n^{\frac{1}{2}}[2k_n h_n + \sinh 2k_n h_n]^{-\frac{1}{2}} \cosh k_n(h_n - y), \tag{2.4}$$

$$\psi_{nj}(y) = 2S_{nj}^{\frac{1}{2}}[2S_{nj} h_n + \sin 2S_{nj} h_n]^{-\frac{1}{2}} \cos S_{nj}(h_n - y), \tag{2.5}$$

$$q_n = (k_n^2 - p^2)^{\frac{1}{2}}, \tag{2.6}$$

$$r_{nj} = (S_{nj}^2 + p^2)^{\frac{1}{2}}, \tag{2.7}$$

$$gk_n \tanh k_n h_n = \sigma_\nu^2 \tag{2.8}$$

and

$$gS_{nj} \tan S_{nj} h_n = -\sigma_\nu^2. \tag{2.9}$$

In this last, the S_{nj} are the ordered positive solutions, so that the index j corresponds to the number of zero-crossings of the ephemeral mode, $\psi_{nj}(y)$. The vertical modes χ_n, ψ_{nj} are orthonormal over the corresponding depth intervals $(0, h_n)$.

As shown elsewhere (e.g. Smith 1983), the matching conditions at $x = 0$ can be written to lowest order as

$$\sigma_1 \phi_1 = \sigma_2 \phi_2, \tag{2.10}$$

$$\sigma_1^{-1} \frac{\partial \phi_1}{\partial x} = \sigma_2^{-1} \frac{\partial \phi_2}{\partial x}, \quad 0 < y < h_1, \tag{2.11}$$

$$\frac{\partial \phi_2}{\partial x} = 0, \quad h_1 < y < h_2. \tag{2.12}$$

The first of these (2.10) ensures continuous pressure; the second (2.11) requires that material on the vortex sheet between the regions remains on the sheet, i.e. continuous horizontal displacements across the boundary; the last (2.12) ensures no flow into or out of the vertical face of the step.

To complete the formulation as in the previous works, the horizontal displacements at $x = 0$ are defined:

$$U(y) = \begin{cases} \sigma_n^{-1} \dfrac{\partial \phi_n}{\partial x}, & 0 < y < h_1, \\ 0, & h_1 < h < h_2. \end{cases} \tag{2.13}$$

The displacement condition (2.11) is convolved over $0 < y < h_n$ with χ_n and the ψ_{nj}, yielding (using the orthonormality)

$$(A_n - B_n) = \frac{\mathrm{i}\sigma_n}{q_n} \int_0^{h_n} U(y)\,\chi_n(y)\,\mathrm{d}y \tag{2.14}$$

and

$$C_{nj} = -\frac{\sigma_n}{r_{nj}} \int_0^{h_n} U(y)\,\psi_{nj}(y)\,\mathrm{d}y. \tag{2.15}$$

Note that this is only possible because $U(y) = 0$ over $h_1 < y < h_2$, so that the $n = 2$

convolutions can be extended to h_2. Substituting (2.15) into (2.10), the pressure condition becomes

$$\sum_{n=1}^{2} (A_n + B_n)\,\sigma_n\,\chi_n(y) = \int_0^{h_1} U(t)\,G(y,t)\,\mathrm{d}t, \quad 0 < y < h_1, \tag{2.16}$$

where

$$G(y,t) \equiv \sum_{n=1}^{2} \sigma_n^2 \sum_{j=1}^{\infty} r_{nj}^{-1}\,\psi_{nj}(t)\,\psi_{nj}(y). \tag{2.17}$$

The problem is thus posed as an integral equation with a symmetric kernel.

The various solutions will be expressed in terms of a transmission matrix $\boldsymbol{T}$, relating outgoing to incident amplitudes:

$$\boldsymbol{B} = \boldsymbol{T}\boldsymbol{A}, \tag{2.18}$$

where

$$\boldsymbol{B} = (B_1, B_2)^{\mathrm{T}}, \quad \boldsymbol{A} = (A_1, A_2)^{\mathrm{T}}. \tag{2.19a, b}$$

For example, the trivial case $h_1 = h_2$ and $V_1 = V_2$ results in the anti-identity matrix because of the way the ϕ_n are defined:

$$\boldsymbol{T} = \begin{bmatrix} 0 & -1 \\ -1 & 0 \end{bmatrix}. \tag{2.20}$$

Although an exact expression for $\boldsymbol{T}$ may be derived from the foregoing (see e.g. Evans 1975), it is simpler here to substitute the trial functions for $U(y)$ from each approximation directly into (2.14) and (2.16), and find the elements of $\boldsymbol{T}$ by elimination. The intermediate results of the more elegant expression are singular for the plane-wave solution (Miles 1967).

As mentioned in §1, action flux perpendicular to the discontinuity is conserved. Smith (1983) showed that the action equation in this case reduces to the form

$$-q_1(|A_1|^2 - |B_1|^2) = q_2(|A_2|^2 - |B_2|^2). \tag{2.21}$$

(Unfortunately, this equation (3.12) in the 1983 paper, was omitted in the published version.)

Finally, to relate the potential amplitudes A_n, B_n to surface displacements a_n, b_n, surface amplitudes are defined as in Miles (1967):

$$(a_n, b_n) \equiv -\mathrm{i}q^{-1}\sigma_n\,\chi_n(0)\,(A_n, B_n) = -\mathrm{i}\left\{\frac{\sigma_n k_n}{g c_n^{\mathrm{g}}}\right\}^{\frac{1}{2}} (A_n, B_n), \tag{2.22}$$

where c_n^{g} is the group velocity in region n. For example, with $a_1 = 1$ and $a_2 = 0$, the surface-amplitude reflection R and transmission T become

$$R_1 = T_{11} \tag{2.23}$$

and

$$T_1 = -T_{21}\left\{\frac{\sigma_2\,\chi_2(0)}{\sigma_1\,\chi_1(0)}\right\}, \tag{2.24}$$

while with $a_1 = 0, a_2 = 1$,

$$R_2 = T_{22} \tag{2.25}$$

and

$$T_2 = -T_{12}\left\{\frac{\sigma_1\,\chi_1(0)}{\sigma_2\,\chi_2(0)}\right\}. \tag{2.26}$$

In general, three classes of solutions can arise: (i) the normal case of simple refraction and partial reflection; (ii) for sufficiently large following currents, $k_{\mathrm{t}}^2 < p^2$, so q_{t} is imaginary and total reflection occurs (where t is the index of the transmitted waves);

and (iii) for extremely large following currents once again $k_t^2 > p^2$, but with $\sigma_t < 0$, and transmission occurs into waves propagating upstream (there can be over-reflection in this case).

3. Some approximations

3.1. *Truncation*

To solve (2.14) and (2.16) explicitly, $U(y)$ is expressed in terms of the truncated orthonormal set (over $0 < y < h_1$) taken from the shallower region (cf. Kirby *et al.* 1987):

$$U(y) = u_0 \chi_1 + \sum_{j=1}^{M} u_j \psi_{1j}. \tag{3.1}$$

Both sides of (2.16) are convolved with each member of this set, leading to $(M+1)$ new equations in its place, with $(M+1)$ new unknowns as well. Note that some number M' of the other set of ephemeral modes ψ_{n2} must also be chosen to evaluate G in (2.17). These need not be equal; in fact, Miles' variational approximation (below) corresponds to $M = 0, M' \to \infty$. The two equations for displacement at the boundary (2.14) reduce the four free-wave amplitudes to a two-parameter family of solutions, depending on the two incident amplitudes as implied in (2.18). Presumably, as M and M' are increased, the solution can be obtained to arbitrary accuracy; this is one approach taken (with $M = M' = 10$) by Kirby *et al.* (1987). Note that as $k_n h_n$ becomes large, it is not necessarily the lowest-mode ψ_{ni} which are important; rather, those modes for which the S_{ni} are comparable to the k_n may dominate in the matching.

3.2. *Plane-wave solution* (P1)

A plane-wave solution (P1) analogous to Lamb's (1945) shallow-water step solution is obtained as by Miles (1967): (3.1) is truncated to

$$U(y) \approx u_0 \chi_1. \tag{3.2}$$

Equation (2.14) then becomes

$$(A_1 - B_1) = \frac{\mathrm{i}\sigma_1}{q_1} u_0, \quad (A_2 - B_2) = \frac{\mathrm{i}\sigma_2}{q_2} (\lambda N)\, u_0, \tag{3.3a, b}$$

and (2.16), with G set to zero, becomes

$$\sigma_1 (A_1 + B_1) + \sigma_2 \lambda N (A_2 + B_2) = 0, \tag{3.4}$$

where

$$\lambda N \equiv \int_0^{h_1} \chi_1 \chi_2 \,\mathrm{d}y, \quad \lambda^2 \equiv \frac{\sigma_1^2 q_2}{\sigma_2^2 q_1}. \tag{3.5a, b}$$

The result, with $L \equiv \sigma_2 \lambda / \sigma_1$, is

$$\boldsymbol{T} = (1+N^2) \begin{bmatrix} (N^2-1) & -2NL \\ -2NL^{-1} & (1-N^2) \end{bmatrix}. \tag{3.6}$$

Figure 2 shows the magnitude of reflection according to P1 (and also by the action-model A, to be discussed later) for waves incident at various angles from deep water onto a shelf, as considered by Miles (1967). In the lower plots, the shelf depth h_1 is normalized by the incident wavenumber, $k_2 \equiv 1.0$; thus, the x-coordinate is directly proportional to the depth. In the upper plots, shelf depth is shown relative to transmitted wavenumber k_1, as in Miles (1967); this is provided for comparison with Miles (1967) and also because it shows an expanded view of the region near $h_1 = 0$.

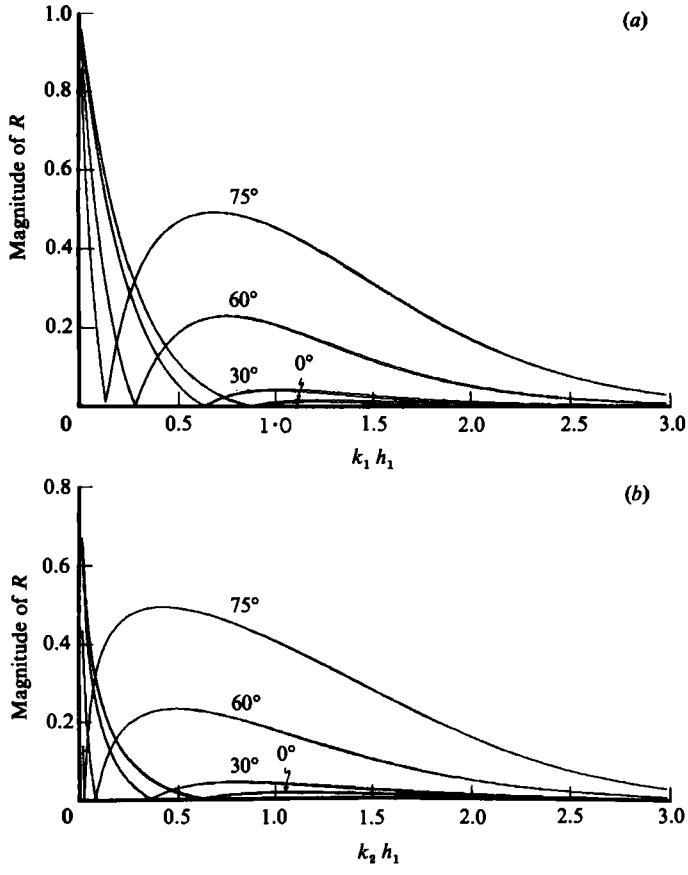

FIGURE 2. Magnitude of reflection from a shelf for waves incident at various angles from deep water. Shelf depth is shown normalized by (*a*) transmitted wavenumber ($k_1 h_1$), as in Miles (1967); and (*b*) $k_2 h_1$ relative to the incident (fixed) wavenumber. Note that (*a*) expands the region of small h_1. Both the plane wave (P1) and the action (A) models are plotted. To the right of the zero-crossing, the A curve is just barely above the P1 curve; otherwise, they are indistinguishable.

The sign of (the real part of) R reverses at finite depth, from positive in the shallow h_1 limit to negative at intermediate depth. A key to understanding this is the group velocity perpendicular to the shelf. Consider first waves normally incident from the deep region (2) into shallow water, where $c^{\mathrm{g}} = c^{\mathrm{p}} = (gh_1)^{\frac{1}{2}}$. As $h_1 \to 0$, c^{g} decreases, so larger amplitudes are required in the shallower region to maintain a constant action flux across the step. Thus, positive reflection aids in matching. Conversely, as h_1 is increased c^{p} increases monotonically, but c^{g} goes from c^{p} to $\frac{1}{2}c^{\mathrm{p}}$ with a maximum at an intermediate depth. For h_1 near this intermediate value, c^{g} is larger than in deep water, so less amplitude is required in region 1 to match the action flux from region 2. In this case negative reflection helps by reducing the amplitude at the boundary. In the case of obliquely incident waves, the decrease in c^{p} in the shallower region turns the waves towards normal, further increasing the component of c^{g} perpendicular to the step; thus this intermediate-depth effect is increased as the angle of incidence increases.

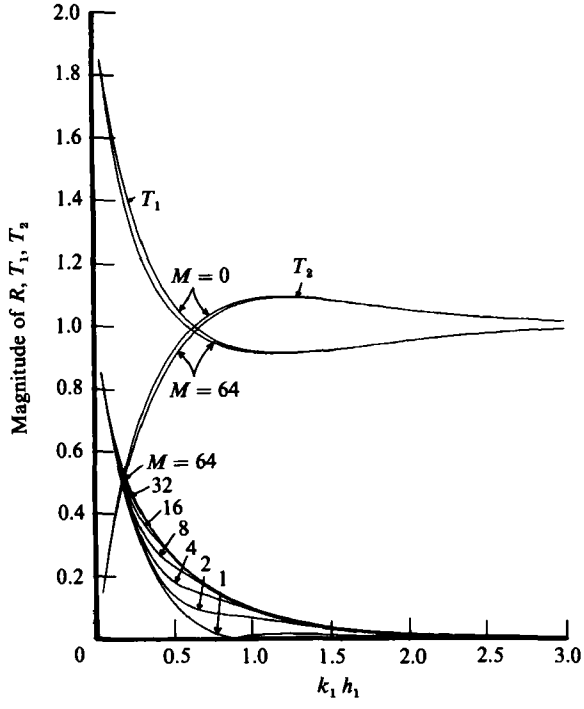

FIGURE 3. Magnitudes of transmission and reflection at 0° incidence by M1, using various numbers of terms M in the trapped-mode contribution. Near $k_1 h_1 = 0.2$, even 32 terms are barely adequate to resolve the reflection. Transmission is shown for $M = 0$ and 64 only; T_1 corresponds to transmission from deep to shallow, T_2 to transmission from shallow to deep.

3.3. *Miles' variational approximation* (M1)

The variational approximation of Miles (1967) is recovered by relaxing the condition $G = 0$. Putting $U(y) \approx u_0 \chi_1$ into (2.16) and convolving with χ_1 over $0 < y < h_1$ yields

$$\sigma_1(A_1+B_1)+\sigma_2\lambda N(A_2+B_2) = u_0 X\left(\frac{\sigma_1^2}{q_1}\right), \tag{3.7}$$

where

$$\begin{aligned} X &\equiv \left(\frac{q_1}{\sigma_1^2}\right)\int_0^{h_1}\int_0^{h_1}\chi_1(y)\,G(y,t)\,\chi_1(t)\,\mathrm{d}y\,\mathrm{d}t, \\ &= q_2\lambda^{-2}\sum_{j=1}^{\infty} r_{2j}^{-1}\left(\int_0^{h_1}\chi_1(y)\,\psi_{2j}(y)\,\mathrm{d}y\right)^2, \\ &= q_2\lambda^{-2}\chi_1^2(0)\sum_{j=1}^{\infty}\frac{r_{2j}^{-1}\psi_{2j}^2(0)}{(k_1^2+S_{2j}^2)^2}\left[g^{-1}(\sigma_1^2-\sigma_2^2)+\frac{S_{2j}\sin S_{2j}(h_2-h_1)}{\cos S_{2j}h_2\cosh k_1 h_1}\right]^2. \end{aligned} \tag{3.8}$$

Together with (3.3) this leads to

$$\boldsymbol{T} = (1+N^2-\mathrm{i}X)^{-1}\begin{bmatrix}(N^2-1-\mathrm{i}X) & -2NL\\ -2NL^{-1} & (1-N^2-\mathrm{i}X)\end{bmatrix}. \tag{3.9}$$

The results, denoted M1, for waves incident from deep water (actually $k_2 h_2 = 4$) onto shelves of various depths are shown in figure 3, using various numbers M of modes in evaluating X via (3.8). Note that $M = 0$ corresponds to P1. Here, the reflection

and transmission are plotted against $k_1 h_1$ to facilitate comparison with M67 and for the expanded view of the shallow-shelf limit. The effect of X is always to increase the magnitude of R relative to the P1 contribution. Also, X smooths over the sign reversal of R seen in P1. Note that the ephemeral modes contribute significantly (via X) to R over depths $k_1 h_1$ near 0.5. Finally, as $k_1 h_1$ decreases more modes are required to fill in the reflection, until even 32 modes are barely adequate near $k_1 h_1 = 0.2$. To understand this, view it in terms of h_1/h_2 rather than $k_1 h_1$: on the deep side, $k_2 h_2 = 4$ and $k_2 \approx \sigma 2/g \equiv$ constant, while on the shallow side, $k_1 h_1 = \frac{1}{5}$ and $k_1 \approx 5(\sigma 2/g) = 5k_2$; thus, $k_2 h_1 = (\frac{1}{5})^2$ and so $h_1/h_2 = \frac{1}{100}$. To resolve h_1 with modes of comparable vertical scale, 100 modes would be required in region 2; in the light of this, it is not surprising that so many modes are required.

3.4. *Flat bottom*: *Evans' approach* (E)

In the case $h_1 = h_2$, convolution of the pressure condition with the $n = 2$ set of functions presents no problem. In this case, the selection $U(y) \sim \chi_1(y)$ seems rather one-sided, and Evans (1975) instead chooses (effectively)

$$U(y) \approx \sum_{n=1}^{2} d_n \chi_n. \tag{3.10}$$

Convolutions with χ_1 and χ_2 lead to

$$\sigma_1(A_1+B_1)+I\sigma_2(A_2+B_2) = \left(\frac{\sigma_1^2}{q_1}\right) X_1 d_1, \tag{3.11a}$$

$$I\sigma_1(A_1+B_1)+\sigma_2(A_2+B_2) = \left(\frac{\sigma_2^2}{q_2}\right) X_2 d_2, \tag{3.11b}$$

where $I \equiv \lambda N$, X_1 is the same as X of (3.8), and X_2 is given by (3.8) with all 1s and 2s reversed and with λ^{-2} replaced by λ^2. The displacement condition yields

$$A_1 - B_1 = \frac{\mathrm{i}\sigma_1}{q_1}(d_1 + Id_2) \tag{3.12a}$$

and

$$A_2 - B_2 = \frac{\mathrm{i}\sigma_2}{q_2}(Id_1 + d_2). \tag{3.12b}$$

After some algebra, the result may be written

$$\boldsymbol{T} = (u_1 u_2 - v_1 v_2)^{-2} \begin{bmatrix} (u_1^* u_2 - v_1^* v_2) & -2(\lambda L)\,\mathrm{Im}\{v_1 u_1^*\} \\ -2(\lambda L)^{-1}\,\mathrm{Im}\{v_2 u_2^*\} & (u_1 u_2^* - v_1 v_2^*) \end{bmatrix}, \tag{3.13}$$

where

$$u_n \equiv \{1 - I^2 - \mathrm{i}X_n\}, \tag{3.14}$$

$$v_1 \equiv I\{1 - I^2 + \mathrm{i}\lambda^{-2}X_2\}, \quad v_2 \equiv I\{1 - I^2 + \mathrm{i}\lambda^2 X_1\}, \tag{3.15a, b}$$

3.5. *Flat bottom, continued* (P2, M2)

Unfortunately, the above approach does not easily generalize to $h_1 < h_2$, since the convolutions of (2.16) are necessarily restricted to the shallower depth, and the functions χ_2, ψ_{2n} are not orthogonal over this range. To assess the prejudice introduced in P1 by (3.2), replace (3.2) with

$$U(y) \approx u_0 \chi_2(y). \tag{3.16}$$

The result is easily worked out by reversing the roles of $n = 1$ and 2, leading to

$$\hat{\boldsymbol{T}} = (\hat{N}^2+1)^{-1} \begin{bmatrix} (1-\hat{N}^2) & -2\hat{N}\hat{L} \\ -2\hat{N}\hat{L}^{-1} & (\hat{N}^2-1) \end{bmatrix}, \tag{3.17}$$

where, with $\hat{\lambda} \equiv \lambda^{-1}$,

$$\hat{L} = \frac{\sigma_1 \hat{\lambda}}{\sigma_2} = \frac{\sigma_1}{\lambda \sigma_2} = L^{-1}, \tag{3.18}$$

and

$$\hat{\lambda}\hat{N} = \int_0^h \chi_1 \chi_2 \, dy = \lambda N. \tag{3.19}$$

By inspection of (3.17), this solution (P2) would match P1 only if $\hat{N} = N^{-1}$; yet from (3.19) this would require $\lambda N = \hat{\lambda}\hat{N} = 1$. A compromise solution, giving just this result, is obtained by replacing (3.5*a*) with

$$\lambda N' \equiv \left[\int_0^{h_1} \chi_1^2 \, dy \int_0^{h_1} \chi_2^2 \, dt \right]^{\frac{1}{2}}, \tag{3.20}$$

where λ is defined as in (3.5*b*). With $h_1 = h_2$, the resulting model corresponds exactly to the 'action-based model' of Smith (1983). The use of h_1 in both integrals here is deliberate, anticipating the next section. Physically (3.5*a*) overemphasizes the mismatch of χ_1 and χ_2, leading to an exaggerated change in the index of refraction N. The substitution (3.20) corresponds to an assumption that the ephemeral modes redistribute the variance of χ_1 and χ_2 vertically, without affecting the impedance at the boundary itself. This strategy is extended to the more general case of a change in depth as well in §3.6.

In a similar fashion, $n = 1$ and 2 can be reversed in Miles' variational improvement, leading to an analogous result, here denoted M2. Comparison and discussion of these various results are given in §4.

3.6. *An action-based model* (A)

In Smith (1983), an unspecified average $\langle \chi_n \rangle$ was posited and, in the case $h_1 = h_2$, assumed to apply equally to the pressure and displacement conditions. This led to equations of the form (in the present notation)

$$-\gamma(A_1 + B_1) = (A_2 + B_2), \tag{3.21}$$

and

$$\alpha\gamma(A_1 - B_1) = (A_2 - B_2), \tag{3.22}$$

where

$$\gamma = \frac{\sigma_1 \langle \chi_1 \rangle}{\sigma_2 \langle \chi_2 \rangle}, \tag{3.23}$$

and

$$\alpha = \frac{\sigma_2^2 q_1}{\sigma_2^2 q_2}. \tag{3.24}$$

This has the general solution

$$\boldsymbol{T} = (1+\alpha)^{-1} \begin{bmatrix} \alpha - 1 & -2\gamma^{-1} \\ -2\alpha\gamma & 1 - \alpha \end{bmatrix}. \tag{3.25}$$

From this, conservation of action (2.21) implies the relation

$$\alpha\gamma^2 = q_1/q_2. \tag{3.26}$$

which, in turn, implies that $\langle \chi_1 \rangle = \langle \chi_2 \rangle$. The results of following the treatment through with non-normalized functions suggests that this average corresponds to a root-mean square over depth,

$$\langle \chi_n \rangle = \left[\int_0^{h_n} \chi_n^2 \, dy \right]^{\frac{1}{2}}. \tag{3.27}$$

As noted by Smith (1983), a change in depth at $x = 0$ implies that the same average must not, in fact, apply to both (2.10) and (2.11). Rather, in the shallow-water limit, the conditions must approach those given by e.g. P1: continuous surface elevation, and continuous mass-flux perpendicular to the change.

To extend the results to $h_1 < h_2$, the pressure average is retained as written in (3.27), leading to

$$\langle \chi_1 \rangle = 1, \quad \langle \chi_2 \rangle = \left[\int_0^{h_1} \chi_2^2(y)\, \mathrm{d}y \right]^{\frac{1}{2}} \equiv H^{\frac{1}{2}}. \tag{3.28}$$

Equations (3.21) and (3.22) are also retained in form, and hence so are the resulting (3.25) and (3.26). However, (3.23) becomes

$$\gamma = \frac{\sigma_1}{H^{\frac{1}{2}} \sigma_2}, \tag{3.29}$$

and α now incorporates the difference between a pressure and displacement average, determined from conservation of action:

$$\alpha = \gamma^{-2} \frac{q_1}{q_2} = H \frac{\sigma_2^2 q_1}{\sigma_1^2 q_2}. \tag{3.30}$$

Since $H \to 1$ as $h_2 \to h_1$, this reduces to the previous action-based model in the case of a change in velocity only.

The relation between the plane-wave solution P1 and this model (A) is clarified by referring again to (3.15):

$$\lambda N' \equiv \left[\int_0^{h_1} \chi_1^2\, \mathrm{d}y \int_0^{h_1} \chi_2^2\, \mathrm{d}y \right]^{\frac{1}{2}} \equiv H^{\frac{1}{2}}. \tag{3.31}$$

Identifying N'^2 with α and $N'(\lambda \sigma_2 / \sigma_1) = N' L$ with γ^{-1}, the two solutions, (3.6) and (3.25), are identical.

Finally, in the shallow-water limit $\chi_n \to h_n^{-\frac{1}{2}}$ and so

$$\lambda N \equiv \int_0^{h_1} \chi_1 \chi_2\, \mathrm{d}y \to (h_1^{-\frac{1}{2}} h_2^{-\frac{1}{2}}) h_1 = H^{\frac{1}{2}} \equiv \lambda N'. \tag{3.32}$$

Thus, the models A and P1 converge in the shallow-water limit. In the numerical results given by Kirby *et al.* (1987) for a trench, this is found to be the limit in which P1 performs best.

4. Comparison of models

For comparison, the various results (P1, M1, E and A) are represented homologously and in terms of amplitudes. Referring to (2.23)–(2.26), the amplitude diffraction matrix $\boldsymbol{\tau}$ can be written for M1:

$$\boldsymbol{\tau} \equiv \begin{bmatrix} R_1 & T_2 \\ T_1 & R_2 \end{bmatrix} = (1 + N^2 - \mathrm{i}X)^{-1} \begin{bmatrix} (N^2 - 1 - \mathrm{i}X) & 2N/Q \\ 2NQ & (1 - N^2 - \mathrm{i}X) \end{bmatrix}, \tag{4.1}$$

where

$$Q \equiv \lambda^{-1} \frac{\chi_2(0)}{\chi_1(0)}, \tag{4.2}$$

and λ is defined by (3.5*b*). The results of P1 are recovered by setting $X = 0$ in this, and A is evaluated with $X = 0$ and also replacing N by N', as defined above.

For a step only, the results of models A and P1 were shown in figure 2. As demonstrated by this figure, there is negligible difference in reflection at any shelf

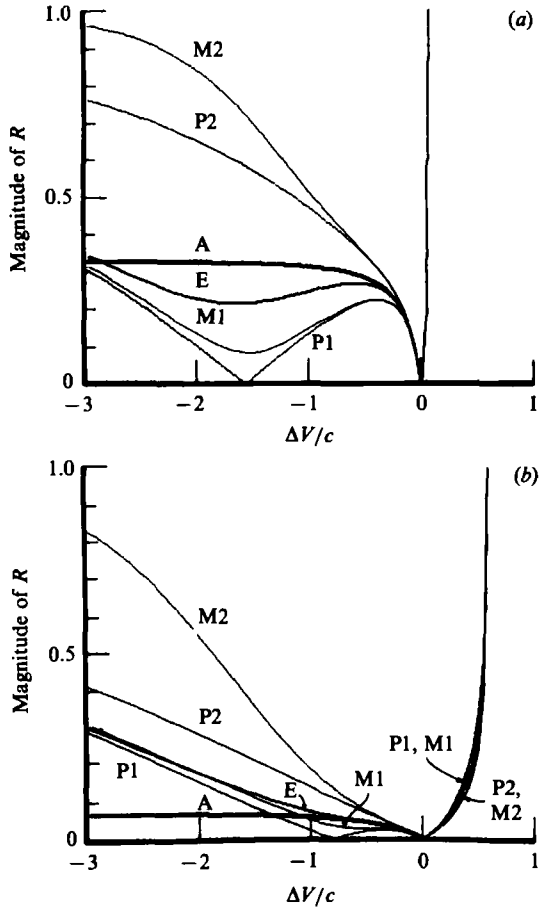

FIGURE 4. Magnitude of reflections from currents alone. The curent change is normalized by the incident phase speed. Evans' (1975) solution (E) is the most accurate. See text for descriptions of the other solutions (action-based A, plane-wave P1 and P2, Miles-like M1 and M2). (*a*) 60° incidence; (*b*) 30°.

depth between these two models. Again, comparison with the variational model (figure 3) indicates that, over a wide range of intermediate depths (measured by $k_1 h_1$), the trapped modes are important.

Next, consider the case of shear alone (Evans' problem). Figure 4 shows the magnitude of reflection in deep water from all 6 models (A, E, P1, P2, M1 and M2), for waves incident at 30° and 60° from normal into a region moving at -3 to $+2$ times the incident phase speed. The results designated P1 and M1 are for waves incident from region 2 (at rest) into region 1 (moving), anticipating the case where waves impinge on a shallower, flowing region from deep water. Conversely, P2 and M2 treat waves incident from region 1 (at rest) into a moving region 2 as would be required for waves impinging on a deeper region in relative motion. The velocity change $\Delta V/c$ is normalized by the incident-wave phase speed. Evans' solution (E) is the most accurate (see McKee & Tesoriero 1986) and is used here as the reference. The next best models are A, M1, and P1. For $|\Delta V/c| < 1$ or so, the action model A compares best with E. For large opposing currents, $\Delta V/c \to -3$, M1 and P1 become more accurate. For the stronger opposing flows ($\Delta V/c < -0.5$ or so), P2 significantly

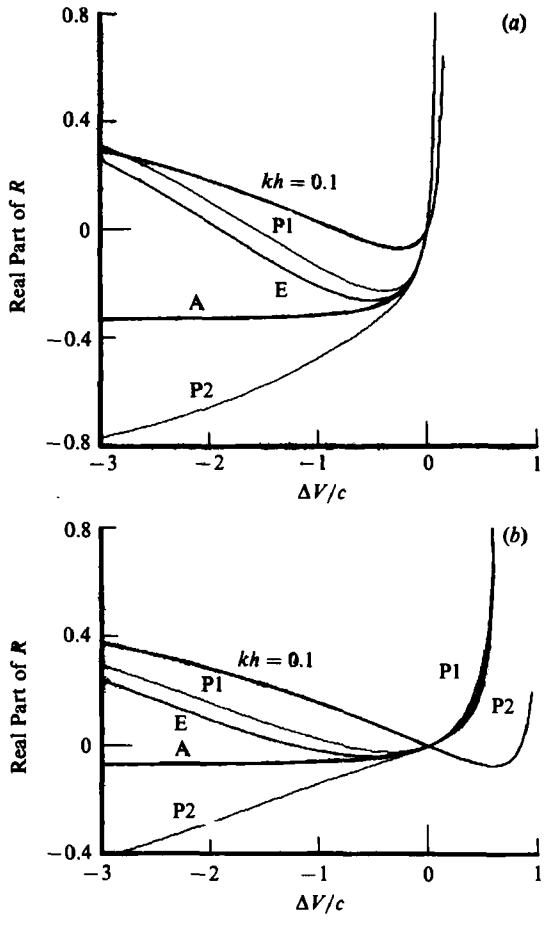

FIGURE 5. Real part of reflections from currents for (*a*) $\theta_1 = 60°$, (*b*) 30°. Note that A is about midway between P1 and P2. The 'reference' reflection E is closest to A for $\Delta V/c > -0.5$, approaches P1 as $\Delta V/c \to -\infty$. For $\Delta V > 0$ in (*b*) (30°), A and E coincide between the values from P1 and P2. In the shallow-wave limit, all models coincide ($kh \leqslant 0.1$).

overpredicts the reflection. Since the trapped modes' contribution in M2 always increases $|R|$, M2 is even worse than P2 in this case.

The step comparison shows the trapped modes' contribution to be important over a wide range of shelf depths, so the poor showing of M2 with current changes implies that none of the approximations given here are suitable for the case of deepening with strong opposing flow. Further, from (4.1), $|R_1| = |R_2|$, so 'deepening with strong opposing flow' is analogous to some dual case of shoaling with following flow. The dual case is found simply by reversing the x-component of the transmitted wave, and renormalizing the change in current by the new incident phase speed. For strong opposing flows, the transmitted wave is refracted toward near-normal exodus, with a much shorter wavelength. The dual in this case corresponds to near-normal incidence with following flow near the turning value (the smallest value yielding total reflection). The best example in figure 4 is for 30° incidence (*b*) near $\Delta V/c = +0.5$ (to the right). Although there is moderate disagreement there, it is no worse than near $\Delta V/c = -0.5$ on the 60° plot (*a*). A general rule is that the approximate solutions are acceptable for $|\Delta V/c| < 0.5$.

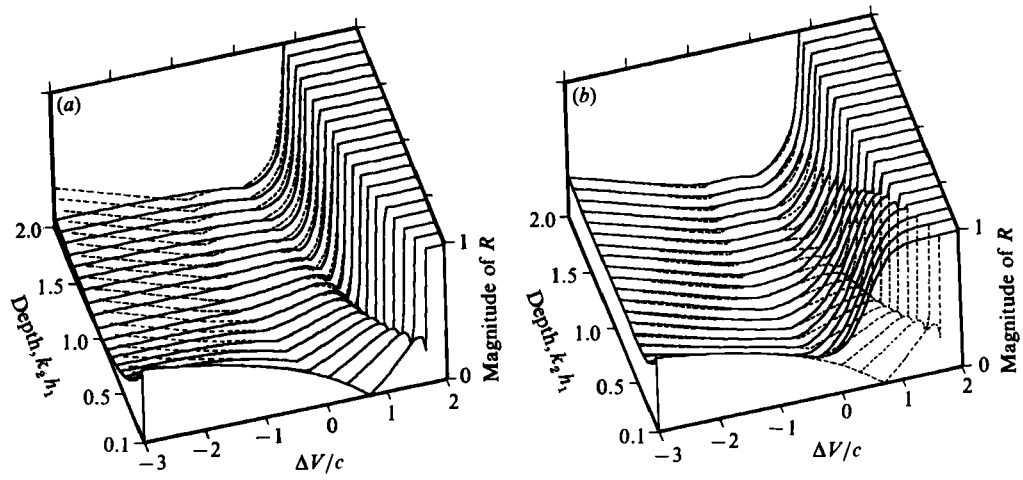

FIGURE 6. (*a*) Comparison of $|R|$ from A (solid lines) and P1 (dashed), and (*b*) comparison of M1 (solid lines) and P1 (dashed), for various currents $\Delta V/c$ (across) and shelf depths $k_2 h_1$ (into page) for waves incident at 30° from deep water ($k_2 h_2 = 4$). For $\Delta V/c > -1$ or so, A and P1 are similar. For $\Delta V/c > 0$, note that M1 > P1 > A. For $k_2 h_1 < 1$ and $\Delta V > 0$, M1 $\gg$ A and P1, indicating that trapped-mode contributions to $|R|$ are significant.

The relation of A to P1 and P2 as a compromise solution is made graphically clear in figure 5, which shows the real part of the reflection (with sign) from the shear alone. The change in index of refraction in model A is roughly the geometric mean of the other two, $N' \approx (N_1 N_2)^{\frac{1}{2}}$, so the reflection by A is midway between P1 and P2. For small currents, and no depth change, the vertical scales on either side are comparable, and this mean solution is appropriate. The pattern of success suggests that as the current increases, a weighted mean would perform better, favouring the smaller-scale profile at the boundary as (in the extreme case) P1 does here. Also shown in figure 5 are the shallow-water limits (for $kh \leqslant 0.1$ or so). In this limit, all the solutions collapse to a single curve. The transition from deep- to shallow-water limits holds no surprises. The deep and shallow curves intersect at (0, 0).

The one-sided approach of P1 and M1 is acceptable whenever the shallower side has the smaller vertical scale, as is certainly the case in the absence of currents. The cases of strong opposing flows and their duals are exceptional in this sense: the region treated as the deeper side has the shorter free-waves, and so can have the smaller vertical scale. Physically, it appears that the ephemeral modes can account more easily for a reduction in vertical scale, so that the actual profile at the boundary favours the smaller-scale profile.

Finally, consider waves incident from deep water onto a shelf, upon which a current flows parallel to the step. Figure 6 shows comparisons, for 30° incidence, between A and P1 (*a*), and between M1 and P1 (*b*). The depth is normalized by the deep-water (incident) wavenumbers $k_2 h_1$. For $|\Delta V/c| < 1$ or so, A and P1 are in rough agreement, which improves with shallower shelfs. In this same velocity range, the M1 *vs.* P1 comparison demonstrates significant contributions from the ephemeral-mode term for $k_2 h_1 < 1$. Much of this region lies to the right of $|\Delta V/c| < 0.5$ and should be viewed with suspicion. Even in the range $0 < \Delta V/c < 0.5$ the difference can be significant. Figure 7 shows the same comparisons for 60° incidence. In this case, agreement

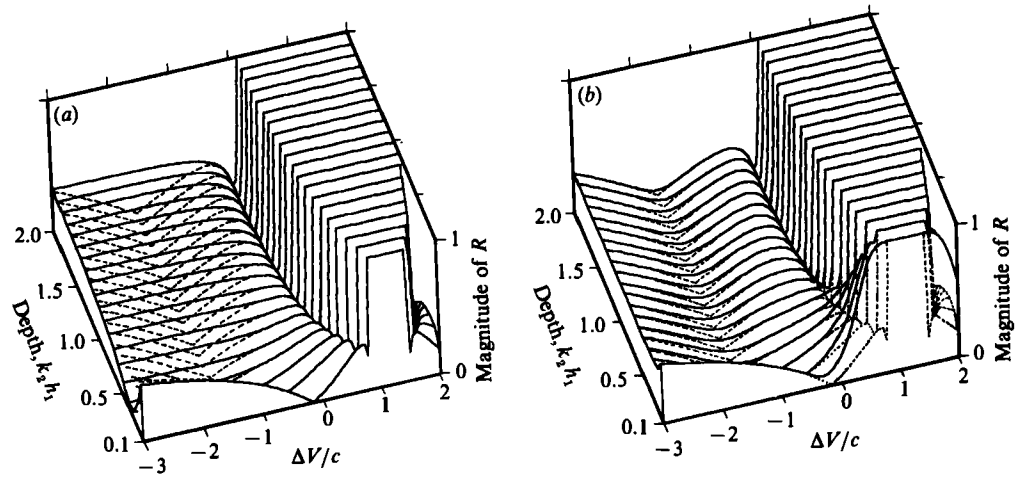

FIGURE 7. As in figure 6, but for $\theta_1 = 60°$. Here, A and P1 (*a*) are virtually coincident for $\Delta V/c > -0.5$. Significant trapped-mode contributions, M1 *vs.* P1, shown in (*b*), are confined to $k_2h_1 < 0.5$ or so. In the lower right-hand corners (small k_2h_1, $\Delta V/c > 1.5$) $|R|$ drops from 1.0 as it becomes possible to match waves propagating upstream.

between A and P1 is restricted to $\Delta V/c > -0.5$, and significant differences between M1 and P1 (i.e. significant trapped contributions) occur only for $k_2h_1 < 0.5$. Also visible in figure 7, for very shallow shelves and extremely strong following currents (lower-right corners) are the class (iii) results with transmissions propagating upstream.

The comparison with M1 indicates that neither of the simpler approximations (A, P1) is adequate to treat significant changes in depth (i.e. transmission onto shelves where $k_2h_1 < \frac{1}{2}$). Even the results of M1 are cast into some doubt for strong following flow, so comparison with a full numerical analysis is desirable (cf. Kirby *et al.* 1987). The pattern of failures strongly suggests that the profile at the discontinuity favours the free waves with smaller vertical scale.

5. Reflection from a partial barrier

Further insight is gained by considering the diffraction by a thin ridge or wall, extending partway up from the bottom. The net diffraction can be obtained from the above for an infinitesimally wide middle region, shallower than the semi-inifinite regions to either side. Referring to the following diagram:

$$\begin{array}{ccccc} A_0 \rightarrow A_2' & \overset{\tau'}{\vdots} & B_1' \rightarrow A_1 & \overset{\tau}{\vdots} & B_2 \rightarrow \\ B_0 \leftarrow B_2' & \underset{x=-D}{\vdots} & A_1' \leftarrow B_1 & \underset{x=0}{\vdots} & A_2 \leftarrow \end{array}, \tag{5.1}$$

the diffraction matrix τ between the middle and right-hand region (at $x = 0$) is just as above. The other matrix τ' is found by shifting to $x' = 0$ *at* $x = -D$ and rotating 180° about the vertical (y-axis). For a wave incident from the left, $A_0 \equiv A_2' \equiv 1$ and $A_2 \equiv 0$. For $D \rightarrow 0$, $B_1' = A_1$ and $A_1' = B_1$ (there is no phase shift). This separation is made simple here because none of the models considered includes ephemeral modes in the shallow (middle) region; rather, a free-wave profile is prescribed. Since the

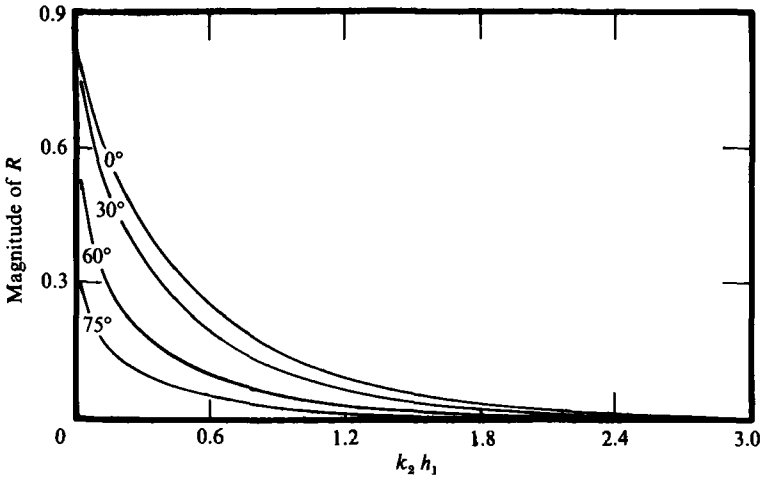

FIGURE 8. Reflection from a submerged wall for various incident angles, for effectively deep water away from the wall ($k_2 h_2 = 4$). Note the rapid drop in $|R|$ as $k_2 h_1$ increases from zero. Only M1 (M2) predicts any reflection here.

inviscid solution is actually singular at the top edge of the wall (Dean 1945), this is a very severe test of the importance of this prescription. The net reflection and transmission are

$$R = (1-\tau_{11}\tau'_{11})^{-1}\tau_{21}\tau_{11}\tau'_{12}+\tau'_{22}, \tag{5.2}$$

and

$$T = (1-\tau_{11}\tau'_{11})^{-1}\tau_{21}\tau'_{12}. \tag{5.3}$$

In the simplest case, $h_0 = h_2$ and $V_0 = V_2$, the problem is symmetric and $\tau = \tau'$; in this case the above reduces to

$$R = -\frac{\mathrm{i}X}{N^2-\mathrm{i}X}, \tag{5.4}$$

and

$$T = \frac{N^2}{N^2-\mathrm{i}X}. \tag{5.5}$$

The resulting reflection *vs.* wall depth is shown in figure 8 for various incident angles.

It is clear from (5.4) that neither P1 nor A predicts any reflection, regardless of the barrier depth. Physically, both solutions employ a tacit assumption that the ephemeral modes are unimportant; i.e. that the reflection is determined entirely by the change in index of refraction N^2. Regardless of the accuracy with which N^2 is estimated, this implies that any reflection R_n from the near face is exactly cancelled by the negative reflection at the far face: $R_f = -R_n$. In this case, the problem reduces entirely to the effects of the ephemeral modes, exactly the opposite of the tacit assumption.

Dean (1945) shows numerically calculated values of $|R|$ for 0° incident angle and two values of $k_2 h_1$. At $k_2 h_1 = \frac{1}{4}$, he shows $|R| = 0.435$, compared with 0.470 from the present variational approximation. At $k_2 h_1 = \frac{1}{2}$, the respective values are 0.267 and 0.302. In both cases, the present result is high by 0.035 times the incident amplitude. While this is worse than an approximation offered by Dean (1945), it is not unreasonable.

6. Summary

A variety of approximate solutions to the general problem of wave diffraction by a change in depth and/or velocity have been presented within a unified framework. The pattern of success among the models shows that the profile at the discontinuity favours the smaller vertical scale, whether this is imposed by the depth or by refraction by a current. This implies that an optimized numerical solution (using as few modes as possible) would probably use more ephemeral modes in regions with larger-scale free waves.

The action model of Smith (1983) was extended to include changes in depth as well as velocity. Mathematically, this model (A) is the geometric mean of the two plane-wave solutions (P1, P2). Physically, the present formulation invites interpretation of model A as an r.m.s. matching over the open portion of the vertical boundary.

The variational approximation of Miles (1967) was extended to include changes in velocity as well as depth. In this approach, the shallower side is assumed to dominate at the boundary, and ephemeral modes on only the deeper side help absorb the difference. Comparison of results with and without contributions from the ephemeral modes indicate these to be important in calculating the reflection from a finite-depth shelf (e.g. deep on one side, $kh < 1$ on the other). This is further emphasized by considering the reflection from a submerged wall (§5): in this case, no reflection is predicted unless the trapped contribution is included.

The two-term Galerkin expansion of Evans (1975) was extended to the finite-depth, flat bottom case (E), but was not extended to changes in depth. For a flat bottom and velocities less than half the incident phase speed, model A is the next best approximation, though in this range all of the models are acceptable. For strong velocities, the vertical profile at the boundary appears to favour the smaller-scale waves, so that one of the one-sided models (M1 or M2) becomes appropriate, while the other (M2 or M1) becomes unacceptable. Thus, the strong surface trapping imposed by greatly reducing the wavelength of the transmitted wave acts very much like a shallower depth; in effect, the waves with larger vertical scale are forced to match the shallower ones.

In the more general case of a change in both depth and current, one or other of the Miles-like solutions (M1 or M2) is available; i.e. that with the ephemeral modes in the deeper region. With no current, the shallower region has waves with smaller scale, so the available solution is the appropriate one. With a current change as well, the smaller-scale waves can result in the deeper region. In this case, it is inferred that none of the models presented here are adequate; rather, a more complete numerical approach is required (cf. Kirby *et al.* 1987). For velocities smaller than half the phase speed, however, this problem is not severe.

The possibility exists (but is not pursued here) that a simple model could be devised by considering a weighted average of P1 and P2; e.g. weighting by the free wavenumbers on either side. Also, the trapped contribution could probably be parameterized in terms of the r.m.s. misfit of the resulting free waves.

This work was supported by Office of Naval Research codes 220 and 420. I also acknowledge useful correspondence with W. D. McKee and J. T. Kirby.

REFERENCES

DEAN, W. R. 1945 On the reflexion of surface waves by a submerged plane barrier. *Proc. Camb. Phil. Soc.* **41**, 231–238.

EVANS, D. V. 1975 The transmission of deep-water waves across a vortex sheet. *J. Fluid Mech.* **68**, 389–401.

HAYES, W. D. 1970 Conservation of action and modal wave action. *Proc. R. Soc. Lond.* A **320**, 187–208.

KIRBY, J. T. 1986 Comments on 'The effects of a jet-like current on gravity waves in shallow water'. *J. Phys. Oceanogr.* **16**, 395–397.

KIRBY, J. T. & DALRYMPLE, R. A. 1983 Propagation of obliquely incident water waves over a trench. *J. Fluid Mech.* **133**, 47–63.

KIRBY, J. T., DALRYMPLE, R. A. & SEO, S. N. 1987 Propagation of obliquely incident water waves over a trench. Part 2. Currents flowing along the trench. *J. Fluid Mech.* **176**, 95–116.

LAMB, H. 1945 *Hydrodynamics*. Dover, 728 pp.

MCKEE, W. D. & TESORIERO, F. 1986 Reflection of water waves from a vertical vortex sheet in water of finite depth. *J. Austral. Math. Soc.* B (submitted).

MEI, C. C. & LO, E. 1984 The effects of a jet-like current on gravity waves in shallow water. *J. Phys. Oceanogr.* **14**, 471–477.

MEI, C. C. & LO, E. 1986 Reply. *J. Phys. Oceanogr.* **16**, 398–399.

MILES, J. W. 1967 Surface-wave scattering matrix for a shelf. *J. Fluid Mech.* **28**, 755–767.

MILES, J. W. 1982 On surface-wave diffraction by a trench. *J. Fluid Mech.* **115**, 315–325.

SMITH, J. 1983 On surface gravity waves crossing weak current jets. *J. Fluid Mech.* **134**, 277–299.